

# Discrimination-aware Network Pruning for Deep Model Compression

Jing Liu, Bohan Zhuang, Zhuangwei Zhuang, Yong Guo, Junzhou Huang, Jinhui Zhu, Mingkui Tan

**Abstract**—We study network pruning which aims to remove redundant channels/kernels and hence speed up the inference of deep networks. Existing pruning methods either train from scratch with sparsity constraints or minimize the reconstruction error between the feature maps of the pre-trained models and the compressed ones. Both strategies suffer from some limitations: the former kind is computationally expensive and difficult to converge, while the latter kind optimizes the reconstruction error but ignores the discriminative power of channels. In this paper, we propose a simple-yet-effective method called discrimination-aware channel pruning (DCP) to choose the channels that actually contribute to the discriminative power. To this end, we first introduce additional discrimination-aware losses into the network to increase the discriminative power of the intermediate layers. Then, we select the most discriminative channels for each layer by considering the discrimination-aware loss and the reconstruction error, simultaneously. We then formulate channel pruning as a sparsity-inducing optimization problem with a convex objective and propose a greedy algorithm to solve the resultant problem. Note that a channel (3D tensor) often consists of a set of kernels (each with a 2D matrix). Besides the redundancy in channels, some kernels in a channel may also be redundant and fail to contribute to the discriminative power of the network, resulting in kernel level redundancy. To solve this, we propose a discrimination-aware kernel pruning (DKP) method to further compress deep networks by removing redundant kernels. To prevent DCP/DKP from selecting redundant channels/kernels, we propose a new adaptive stopping condition, which helps to automatically determine the number of selected channels/kernels and often results in more compact models with better performance. Extensive experiments on both image classification and face recognition demonstrate the effectiveness of our methods. For example, on ILSVRC-12, the resultant ResNet-50 model with 30% reduction of channels even outperforms the baseline model by 0.36% in terms of Top-1 accuracy. The pruned MobileNetV1 and MobileNetV2 achieve  $1.93\times$  and  $1.42\times$  inference acceleration on a mobile device, respectively, with negligible performance degradation. The source code and the pre-trained models are available at <https://github.com/SCUT-AILab/DCP>.

**Index Terms**—Channel Pruning, Kernel Pruning, Network Compression, Deep Neural Networks.

## I. INTRODUCTION

**S**INCE 2012, deep neural networks (DNNs) have achieved great success in many computer vision tasks, *e.g.*, image classification [23], [38], [67], face recognition [9], [61], [68],

Jing Liu, Zhuangwei Zhuang, Yong Guo, Jinhui Zhu, and Mingkui Tan are with the School of Software Engineering, South China University of Technology. E-mail: {seliujing, z.zhuangwei, guo.yong}@mail.scut.edu.cn, {csjhzhu, mingkuitan}@scut.edu.cn.

Bohan Zhuang is with the School of Computer Science, The University of Adelaide, Australia; and the Australian Centre for Robotic Vision. E-mail: bohan.zhuang@adelaide.edu.au.

Junzhou Huang is with the Computer Science and Engineering department, The University of Texas at Arlington. E-mail: jzhuang@uta.edu

image generation [5], [13], [15], video analysis [63], [76], [83] and many other areas [14], [20]. However, the large model size and high computation cost remain great obstacles for many applications, especially on some constrained devices with limited memory and computational resources. To address this problem, model compression is an effective approach, which aims to reduce the model redundancy without significant degeneration in performance.

Recent studies on model compression mainly contain three categories, namely, quantization [21], [59], [85], sparse or low-rank compression [18], [21], [84], and network pruning [47], [51], [79], [81]. Network quantization seeks to represent weights and activations with low bitwidth fixed-point integers; thus convolution operations can be implemented by efficient XNOR-popcount bitwise operations for substantial speed-up. However, the training can be very difficult since the non-differentiable quantizer that transforms the continuous weights/activations into the discrete ones would inevitably bring errors and hamper the model performance [59]. Sparse connections methods can obtain high compression rate in theory, but they may generate irregular convolutional kernels that need carefully designed sparse matrix operations. Low-rank compression methods seek to approximate the original filters of a pre-trained model with low-rank filters. Nevertheless, they are often inefficient for the convolutions with small kernels sizes, *e.g.*,  $1\times 1$  [70]. In contrast, network pruning reduces the model size and speeds up the inference by removing the redundant modules (channels [27], [47], [90] or kernels [2], [53]). In particular, channel pruning can be well supported by existing deep libraries with little additional effort compared with network quantization and sparse or low-rank connections. More critically, most compression methods, such as quantization, can be easily applied on top of network pruning. For example, pruning redundant channels/kernels is able to further accelerate the inference speed of the quantized models by reducing the number of parameters [21].

In network pruning, how to identify the informative (or important) channels/kernels, also known as channel/kernel selection, has become an important problem. Existing methods can be divided into two categories, namely, training-from-scratch methods [1], [47], [77] and reconstruction-based methods [27], [29], [41], [51]. Training-from-scratch methods directly learn the importance of channels/kernels with sparsity regularization, but it is very difficult to train very deep networks on large-scale data sets [1], [47]. For the reconstruction-based methods, they seek to perform network pruning by minimizing the reconstruction error of feature maps between the pruned model and the pre-trained one [27], [51]. These methods suffer

from a critical limitation: the redundant channels/kernels may be mistakenly kept to minimize the reconstruction error of feature maps. Consequently, these methods may incur severe performance degradation on more compact and deeper models, such as MobileNet [28] for large-scale data sets.

In this paper, we aim to overcome the drawbacks of both strategies. In contrast to existing methods [27], [29], [41], [51], we assume and highlight that an informative channel/kernel, no matter where it is, should own sufficient discriminative power; otherwise, it should be removed. Based on this intuition, we propose a discrimination-aware channel pruning (DCP) method to find the channels that actually contribute to the discriminative power of the network. In DCP, relying on a pre-trained model, we first introduce multiple additional discrimination-aware losses into the network to increase the discriminative power of the intermediate layers. Then, we perform channel selection to select the most discriminative channels for each layer by considering both the discrimination-aware loss and the reconstruction error of feature maps. In this way, we are able to make a balance between the discriminative power of the channels and the feature map reconstruction. Note that a channel (3D tensor) consist of kernels (each with a 2D matrix). Some kernels in the selected channels may be redundant and fail to contribute to the discriminative power of the network, which leads to kernel level redundancy. To solve this issue, we propose a discrimination-aware kernel pruning (DKP) method to find the kernels with discriminative power.

Our main contributions are summarized as follows.

- We propose a discrimination-aware channel/kernel pruning (DCP/DKP) scheme to compress deep models with the introduction of additional discrimination-aware losses. The proposed methods first fine-tune the model with the additional losses and the final objective. Then, we conduct channel/kernel selection by simultaneously considering the additional loss and the reconstruction error of feature maps. In this way, the proposed method is able to find the channels/kernels that truly contribute to the discriminative power of the network.
- We formulate the channel/kernel selection problem as an  $\ell_{2,0}$ -norm constrained optimization problem and propose a greedy method to solve the resultant convex optimization problem.
- To prevent DCP/DKP from selecting redundant channels/kernels, we propose a new adaptive stopping condition, which helps to automatically determine the number of selected channels/kernels and often results in more compact models with better performance.
- Extensive experiments demonstrate the superior performance of our methods on a variety of architectures. For example, on ILSVRC-12 [8], when pruning 30% channels of ResNet-50, DCP improves the original model by 0.36% in terms of Top-1 accuracy. we further deploy the pruned models on a smartphone (equipped with a Qualcomm Snapdragon 845 processor). On the mobile CPU, the pruned MobileNetV1 and MobileNetV2 yield negligible performance degradation while achieving significant inference acceleration, *i.e.*,  $1.93\times$  and  $1.42\times$  speedup, respectively.

This paper extends our preliminary version [90] that has been published in NeurIPS 2018 from several aspects. 1) We propose several training techniques to reduce the computational overhead of DCP while still maintaining comparable or even better performance. 2) We apply the improved DCP to more compact models (*i.e.*, MobileNetV1 and MobileNetV2) and achieve state-of-the-art performance on ILSVRC-12. We further deploy the pruned models on a smartphone to investigate the inference acceleration. 3) We apply the improved DCP to compress the latest face recognition models. 4) We extend DCP for kernel pruning to further compress models in the kernel-level. 5) We propose a new adaptive stopping condition for the optimization. 6) We provide more ablative studies to investigate the effectiveness of our methods.

## II. RELATED WORK

**Network quantization.** Quantization-based methods represent the network weights and/or activations with very low precision, which yields highly compact DNNs compared to their floating-point counterparts. The extreme case is the binary neural networks (BNNs) where both weights and activations are constrained to  $\{+1, -1\}$  [4], [31], [59]. In this way, we can replace the matrix multiplication operations with the light-weighted bitwise XNOR-popcount operations. As a result, the 1-bit convolutional layer can achieve up to  $32\times$  memory saving and  $58\times$  speedup on CPUs [59], [89]. However, BNNs still suffer from significant accuracy decreases compared with the full precision counterparts. To reduce this accuracy gap, fixed-point methods have been proposed to represent weights and activations with higher bitwidth. Uniform fixed-point approaches [86], [88] design quantizers with a constant quantization step. To improve the precision of the discrete uniform quantizer, [7], [35] explicitly parameterize and optimize the quantization intervals.

**Sparse or low-rank connections.** To reduce the storage requirements of neural networks, Han *et al.* suggest that neurons with zero input or output connections can be safely removed from the network [22]. With the help of the  $\ell_1/\ell_2$  regularization, weights are pushed to zeros during training. Subsequently, the compression rate of AlexNet can reach  $35\times$  with the combination of pruning, quantization, and Huffman coding [21]. Considering the importance of parameters that are changed during weight pruning, Guo *et al.* propose dynamic network surgery (DNS) in [18]. Training with sparsity constraints [66], [77] has also been studied to reach a higher compression rate. Deep models often contain a lot of correlations among channels. To remove such redundancy, low-rank approximation approaches have been widely studied [11], [12], [33], [65]. For example, Zhang *et al.* speed up VGGNet for  $4\times$  with negligible performance degradation on ILSVRC-12 [84]. However, low-rank approximation approaches are not efficient for the convolutions with small kernels size, *e.g.*,  $1\times 1$  kernel [70].

**Network pruning.** Network pruning aims at removing redundant modules, *e.g.*, channels or kernels, to accelerating the run-time inference speed. As a result, the pruned models would have fewer parameters and lower computational cost.

In order to measure the importance of network module, different metrics [26], [29], [40], [41], [58], [80] are proposed. With a sparsity regularizer in the objective function, training-based methods [1], [47], [77] are proposed to learn the compact models in the training phase. With the consideration of efficiency, reconstruction-methods [27], [29], [41], [51] transform the channel selection problem into the optimization of the reconstruction error. Apart from these methods, the pruning ratio for each layer can also be automatically determined by reinforcement learning [25], [71] or meta-learning [48]. Unlike these methods, DCP focuses on selecting those channels/kernels that actually contribute to the discriminative power of deep networks. Moreover, DCP uses the adaptive stopping conditions to automatically determine the sparsity for each layer.

### III. PROPOSED METHOD

Let  $\{\mathbf{x}_i, y_i\}_{i=1}^N$  be the training samples, where  $N$  indicates the number of samples. Given an  $L$ -layer deep network  $M$ , let  $\mathbf{W} \in \mathbb{R}^{n \times c \times h_f \times z_f}$  represents the model parameters w.r.t. the  $l$ -th convolutional layer (or block). Here,  $h_f$  and  $z_f$  denote the height and width of the filters, respectively;  $c$  and  $n$  denote the number of **input** and **output** channels, respectively. The parameter  $\mathbf{W}$  contains  $n \times c$  kernels in total. Each kernel, for example, the kernel  $\mathbf{W}_{j,k} \in \mathbb{R}^{h_f \times z_f}$  w.r.t. the  $k$ -th input channel and  $j$ -th filter is a matrix with the dimension of  $h_f \times z_f$ . Let  $\mathbf{X} \in \mathbb{R}^{N \times c \times h_{in} \times z_{in}}$  and  $\mathbf{O} \in \mathbb{R}^{N \times n \times h_{out} \times z_{out}}$  be the input feature maps and the involved output feature maps, respectively. Here,  $h_{in}$  and  $z_{in}$  denote the height and width of the input feature maps, respectively;  $h_{out}$  and  $z_{out}$  represent the height and width of the output feature maps, respectively. Moreover, let  $\mathbf{X}_{i,k} \in \mathbb{R}^{h_{in} \times z_{in}}$  be the feature map of the  $k$ -th channel for the  $i$ -th sample. The output feature map of the  $j$ -th channel for the  $i$ -th sample, denoted by  $\mathbf{O}_{i,j} \in \mathbb{R}^{h_{out} \times z_{out}}$ , is computed by

$$\mathbf{O}_{i,j} = \sum_{k=1}^c \mathbf{X}_{i,k} * \mathbf{W}_{j,k}, \quad (1)$$

where  $*$  denotes the convolutional operation.

Given a pre-trained model  $M$ , the task of **Channel Pruning** is to prune those redundant channels in  $\mathbf{W}$  to save the model size and accelerate the inference speed in Eq. (1). In order to choose channels, we introduce a variant of  $\ell_{2,0}$ -norm  $\|\mathbf{W}\|_{2,0} = \sum_{k=1}^c \Omega(\sum_{j=1}^n \|\mathbf{W}_{j,k}\|_F)$ , where  $\Omega(a) = 1$  if  $a \neq 0$  and  $\Omega(a) = 0$  if  $a = 0$ , and  $\|\cdot\|_F$  represents the Frobenius norm. To induce sparsity, we can impose an  $\ell_{2,0}$ -norm constraint on  $\mathbf{W}$ :

$$\|\mathbf{W}\|_{2,0} = \sum_{k=1}^c \Omega\left(\sum_{j=1}^n \|\mathbf{W}_{j,k}\|_F\right) \leq \kappa_c^l, \quad (2)$$

where  $\kappa_c^l$  denotes the desired number of channels at the layer  $l$ . Or equivalently, given a predefined pruning rate  $\eta \in (0, 1)$ , it follows that  $\kappa_c^l = \lceil (1 - \eta)c \rceil$ . When some channels of  $\mathbf{W}$  are removed, the computation w.r.t. these channels can be effectively avoided. As a result, the pruned models would have fewer parameters and lower computational cost than the original models.

#### A. Motivation

Given a pre-trained model  $M^b$ , existing methods [27], [51] conduct channel pruning by minimizing the reconstruction error of feature maps between the pre-trained model  $M^b$  and the pruned one. Formally, the reconstruction error can be measured by the mean squared error (MSE) between the feature maps of the baseline network and the pruned one as follows:

$$\mathcal{L}_M(\mathbf{W}) = \frac{1}{2N \cdot n \cdot h_{out} \cdot z_{out}} \sum_{i=1}^N \sum_{j=1}^n \|\mathbf{O}_{i,j}^b - \mathbf{O}_{i,j}\|_F^2, \quad (3)$$

where  $\mathbf{O}_{i,j}^b \in \mathbb{R}^{h_{out} \times z_{out}}$  denotes the feature maps of  $M^b$ .

Reconstructing feature maps can preserve most information in the learned model, but it has two limitations. First, the pruning performance is highly affected by the quality of the pre-trained model  $M^b$ . If the baseline model is not well trained, the pruning performance can be very limited. Second, to achieve the minimal reconstruction error, some channels in the intermediate layers may be mistakenly kept, even though they are actually irrelevant to the discriminative power of the network. This issue will be even severer when the network becomes deeper.

In this paper, we seek to perform channel pruning by keeping those channels that actually contribute to the discriminative power of the network. In practice, however, it is very difficult to measure the discriminative power of channels due to the complex operations (such as ReLU activation and Batch Normalization) in CNNs. One may consider one channel as an important one if the final loss  $\mathcal{L}_f$  would sharply increase without it. However, for deep models, its shallow layers often have little discriminative power due to the long path of propagation. As a result, it is not practical to evaluate the discriminative power when the network is very deep.

To increase the discriminative power of the intermediate layers, one can introduce additional losses to the intermediate layers of the deep networks [16], [39], [69]. In this paper, we insert  $P$  discrimination-aware losses  $\{\mathcal{L}_S^p\}_{p=1}^P$  evenly into the network, as shown in Figure 1. Let  $\{L_1, \dots, L_P, L_{P+1}\}$  be the layers at which we put the losses, with  $L_{P+1} = L$  being the final layer. For the  $p$ -th loss  $\mathcal{L}_S^p$ , we consider performing channel pruning for the layers  $l \in \{L_{p-1} + 1, \dots, L_p\}$ , where  $L_{p-1} = 0$  if  $p = 1$ . It is worth mentioning that, we can add one loss to each layer of the network, where we have  $L_l = l$ . However, this can be very computationally expensive yet not necessary.

#### B. Construction of discrimination-aware loss

The construction of discrimination-aware loss  $\mathcal{L}_S^p$  is very important in our method. As shown in Figure 1,  $\mathcal{L}_S^p$  uses the output of layer  $L_p$  as the input feature maps. To make the computation of the loss feasible, we impose an average pooling operation over the feature maps. Moreover, to accelerate the convergence, we apply batch normalization [17], [32] and ReLU [55] before performing the average pooling. In this way, the input feature maps for the loss at layer  $L_p$ , denoted by  $\mathbf{F}^p(\mathbf{W})$ , can be computed by

$$\mathbf{F}^p(\mathbf{W}) = \text{AvgPooling}(\text{ReLU}(\text{BN}(\mathbf{O}^p))), \quad (4)$$

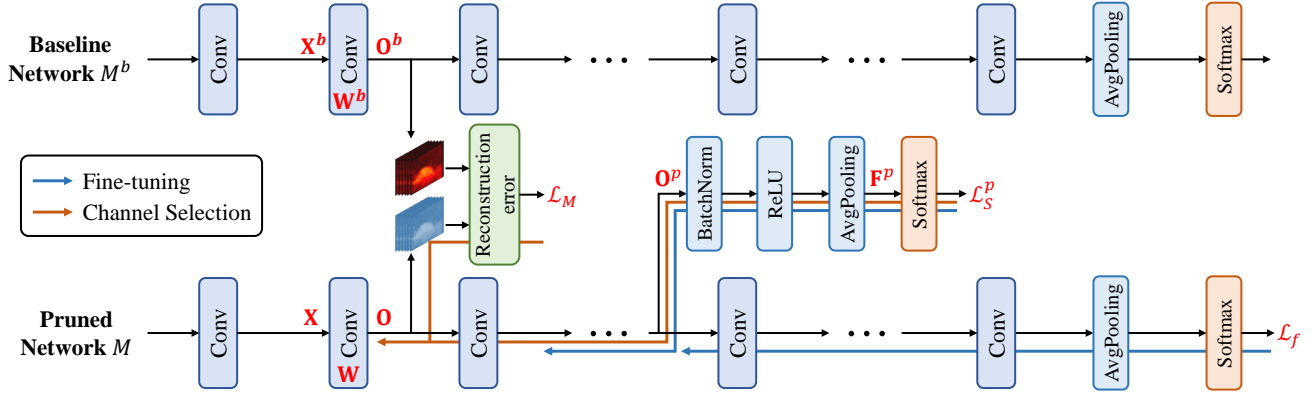


Fig. 1. Illustration of discrimination-aware channel pruning. Here,  $\mathcal{L}_S^p$  denotes the discrimination-aware loss (e.g., cross-entropy loss or additive angular margin loss) in the  $L_p$ -th layer,  $\mathcal{L}_M$  denotes the reconstruction loss, and  $\mathcal{L}_f$  denotes the final loss. DCP first updates the model  $M$  and learns the parameters  $\{\theta^p\}_{p=1}^P$  with  $\{\mathcal{L}_S^p\}_{p=1}^P$  and  $\mathcal{L}_f$ . Then, DCP performs channel pruning with  $P+1$  stages. At each stage, for example, in the  $p$ -th stage, DCP conducts the channel selection for each layer in  $\{L_{p-1}+1, \dots, L_p\}$  with the corresponding  $\mathcal{L}_S^p$  and  $\mathcal{L}_M$ .

where  $\mathbf{O}^p$  represents the output feature maps of layer  $L_p$ . Let  $\mathbf{F}^{(p,i)}$  be the feature maps w.r.t. the  $i$ -th example. The discrimination-aware loss w.r.t. the  $p$ -th loss is formulated as

$$\mathcal{L}_S^p(\mathbf{W}) = -\frac{1}{N} \left[ \sum_{i=1}^N \sum_{t=1}^m I\{y^{(i)} = t\} \log \frac{e^{\theta_t^p \top \mathbf{F}^{(p,i)}}}{\sum_{k=1}^m e^{\theta_k^p \top \mathbf{F}^{(p,i)}}} \right], \quad (5)$$

where  $I\{\cdot\}$  is the indicator function,  $\theta^p \in \mathbb{R}^{n_p \times m}$  denotes the classifier weights of the fully connected layer,  $n_p$  denotes the number of input channels of the fully connected layer and  $m$  is the number of classes. Note that we can also use other losses as the additional loss, such as the additive angular margin loss [9]. (See results in Section V-B).

### C. Discrimination-aware channel pruning

By introducing  $P$  losses  $\{\mathcal{L}_S^p\}_{p=1}^P$  to the intermediate layers, the proposed discrimination-aware channel pruning (DCP) method is shown in Algorithm 1. Starting from a pre-trained model  $M^b$ , DCP first updates the model  $M$  and learns the parameters  $\{\theta^p\}_{p=1}^P$ . Then, DCP performs channel pruning with  $(P+1)$  stages. Algorithm 1 is called discrimination-aware in the sense that the additional losses and the final loss are considered to fine-tune the model. Moreover, the additional losses will be used to select channels, as discussed below.

At the beginning of channel pruning, we first construct additional losses  $\{\mathcal{L}_S^p\}_{p=1}^P$  and insert them at layer  $\{L_1, \dots, L_P\}$  (See Figure 1). Next, we learn the parameters  $\{\theta^p\}_{p=1}^P$  and fine-tune the model  $M$  at the same time with both the additional losses  $\{\mathcal{L}_S^p\}_{p=1}^P$  and the final loss  $\mathcal{L}_f$ . During fine-tuning, all the parameters in  $M$  will be updated. Here, with the fine-tuning, the parameters regarding the additional losses can be well learned.<sup>1</sup> After fine-tuning with  $\{\mathcal{L}_S^p\}_{p=1}^P$  and  $\mathcal{L}_f$ , the discriminative power of the intermediate layers can be significantly improved. Then, we initialize the baseline model  $M^b$  with the fine-tuned model  $M$  and perform channel pruning with  $(P+1)$  stages. At each stage, for example, in the  $p$ -th stage, we conduct channel selection for the layers in  $\{L_{p-1}+1, \dots, L_p\}$  with corresponding  $\mathcal{L}_S^p$  and  $\mathcal{L}_M$ .

<sup>1</sup>The details of the fine-tuning algorithm can be found in [16].

### Algorithm 1 Discrimination-aware channel pruning

**Input:** Pre-trained model  $M^b$ , training data  $\{\mathbf{x}_i, y_i\}_{i=1}^N$ , and hyper-parameters  $\{\kappa_c^l\}_{l=1}^L$ .  
**Output:** Pruned model  $M$ .  
1: Initialize  $M$  using  $M^b$ .  
2: Insert additional losses  $\{\mathcal{L}_S^p\}_{p=1}^P$  to layers  $\{L_1, \dots, L_P\}$ , respectively.  
3: Learn  $\{\theta^p\}_{p=1}^P$  and **Fine-tune**  $M$  with  $\{\mathcal{L}_S^p\}_{p=1}^P$  and  $\mathcal{L}_f$ .  
4: Initialize  $M^b$  using  $M$ .  
5: **for**  $p \in \{1, \dots, P+1\}$  **do**  
6:     **for**  $l \in \{L_{p-1}+1, \dots, L_p\}$  **do**  
7:         Do **Channel Selection** for layer  $l$  using Algorithm 2.  
8:     **end for**  
9: **end for**

### D. Optimization problem for DCP

Since a pre-trained model contains very rich information about the learning task, similar to [51], we hope to reconstruct the feature maps in the pre-trained model. By considering both discrimination-aware loss and reconstruction error, we have a joint loss function as follows:

$$\mathcal{L}(\mathbf{W}) = \lambda \mathcal{L}_M(\mathbf{W}) + \mathcal{L}_S^p(\mathbf{W}), \quad (6)$$

where  $\lambda$  balances the two terms.

**Proposition 1. (Convexity of the loss function)** Let  $\mathbf{W}$  be the model parameters of a considered layer. Given the mean square loss and the discrimination-aware loss defined in Eqs. (3) and (5), the joint loss function  $\mathcal{L}(\mathbf{W})$  is convex w.r.t.  $\mathbf{W}$ .<sup>2</sup>

By introducing the  $\ell_{2,0}$ -norm constraint, the optimization problem for discrimination-aware channel pruning becomes

$$\min_{\mathbf{W}} \mathcal{L}(\mathbf{W}), \quad \text{s.t. } \|\mathbf{W}\|_{2,0} \leq \kappa_c^l, \quad (7)$$

where  $\kappa_c^l$  is the number of channels to be selected. In our method, the sparsity of  $\mathbf{W}$  can be either determined by a pre-defined pruning rate (See Section III) or automatically adjusted by the adaptive stopping conditions in Section III-F.

<sup>2</sup>The proof can be found in Section 7 in [90].

---

**Algorithm 2** Greedy algorithm for channel selection
 

---

**Input:** Training data  $\{\mathbf{x}_i, y_i\}_{i=1}^N$ , model  $M$ , hyperparameters  $\kappa_c^l, \epsilon$ .

**Output:** Selected channel index set  $\mathcal{A}$  and model parameters  $\mathbf{W}_{\mathcal{A}}$ .

- 1: Initialize  $\mathcal{A}_0 \leftarrow \emptyset$ ,  $\mathbf{W}^0 = \mathbf{0}$ , and  $t = 1$ .
- 2: **while** (stopping conditions are not achieved) **do**
- 3:   Compute gradients of  $\mathcal{L}$  w.r.t.  $\mathbf{W}^{t-1}$ :  $\mathbf{G}^{t-1} = \partial\mathcal{L}/\partial\mathbf{W}^{t-1}$ .
- 4:   Find the  $B$  largest  $\|\mathbf{G}_{:,k}^{t-1}\|_F$  and record their indices in  $\mathcal{J}_t$ .
- 5:   Let  $\mathcal{A}_t \leftarrow \mathcal{A}_{t-1} \cup \mathcal{J}_t$ .
- 6:   Solve the following Subproblem to update  $\mathbf{W}_{\mathcal{A}_t}^{t-1}$ :

$$\min_{\mathbf{W}^{t-1}} \mathcal{L}(\mathbf{W}^{t-1}), \text{ s.t. } \mathbf{W}_{\mathcal{A}_t^c}^{t-1} = \mathbf{0}. \quad (8)$$

- 7:   Set  $\mathbf{W}^t \leftarrow \mathbf{W}^{t-1}$  and let  $t \leftarrow t + 1$ .
  - 8: **end while**
- 

### E. Greedy algorithm for channel selection

Due to the non-convexity of  $\ell_{2,0}$ -norm, directly optimizing Problem (7) is very difficult. To address this issue, following the general greedy methods in [3], [45], [72], [73], [82], we propose a greedy algorithm to solve Problem (7).

We show the details of the proposed greedy algorithm in Algorithm 2. At the beginning of the channel selection, we remove all the channels by setting  $\mathbf{W}^0 = \mathbf{0}$ . In each iteration, we first select those channels that actually contribute to the discriminative power of the network. Then, we solve Subproblem (8) with the selected channels only. We will give the details of selecting the channels with discriminative power and the subproblem optimization in the following subsections.

1) *Discrimination-aware channel selection:* At each iteration of Algorithm 2, we compute the gradients  $\mathbf{G}_{:,k}^{t-1} = \partial\mathcal{L}/\partial\mathbf{W}_{:,k}^{t-1}$ , where  $\mathbf{W}_{:,k}^{t-1}$  denotes the parameters for the  $k$ -th input channel at iteration  $t$ . Since we set  $\mathbf{W}^0 = \mathbf{0}$  at the beginning of channel selection, the initial loss value will be very large. Apparently, selecting any channel at  $t$ -th iteration will decrease the loss function, and the channel with the largest gradient  $\|\mathbf{G}_{:,k}^{t-1}\|_F$  will decrease the loss function the most. With this selection criteria, we choose  $B$  channels corresponding to the  $B$  largest  $\|\mathbf{G}_{:,k}^{t-1}\|_F$  as active channels and record their indices into  $\mathcal{J}_t$ .

Let  $\mathcal{A}_t \subset \{1, \dots, c\}$  be the index set of the selected channels up to iteration  $t$ , i.e.,  $\mathcal{A}_t = \cup_i \mathcal{J}_i, i = 1, \dots, t$ . In general, once a channel is added into  $\mathcal{J}_t$ , it is unlikely to be selected in the following iteration. However, if we do not solve Subproblem (8) accurately, some of the selected channels may have large value of  $\|\mathbf{G}_{:,k}^{t-1}\|_F$ , thus they might be chosen again. To avoid this issue, we propose choosing channels from  $\{1, \dots, c\} \setminus \mathcal{A}_{t-1}$  to form  $\mathcal{J}_t$ . In this way, there will be no overlapping channels among  $\mathcal{J}_i$ 's, where  $i = 1, \dots, t$ .

2) *Subproblem optimization:* Once  $\mathcal{A}_t$  is determined, we optimize  $\mathbf{W}^{t-1}$  w.r.t. the selected channels by minimizing Subproblem (8). Here,  $\mathbf{W}_{\mathcal{A}_t^c}^{t-1}$  denotes the subtensor indexed by  $\mathcal{A}_t^c$ , and  $\mathcal{A}_t^c$  is the complementary set of  $\mathcal{A}_t$ , i.e.,  $\mathcal{A}_t^c = \{1, \dots, c\} \setminus \mathcal{A}_t$ .

To solve the Subproblem in Eq. (8), we apply stochastic gradient descent (SGD) and update  $\mathbf{W}_{\mathcal{A}_t}^{t-1}$  by

$$\mathbf{W}_{\mathcal{A}_t}^{t-1} \leftarrow \mathbf{W}_{\mathcal{A}_t}^{t-1} - \gamma \frac{\partial\mathcal{L}}{\partial\mathbf{W}_{\mathcal{A}_t}^{t-1}}, \quad (9)$$

where  $\mathbf{W}_{\mathcal{A}_t}^{t-1}$  denotes the subtensor indexed by  $\mathcal{A}_t$ , and  $\gamma$  denotes the learning rate.

Note that when optimizing Subproblem (8),  $\mathbf{W}_{\mathcal{A}_t}^{t-1}$  is warm-started from the fine-tuned model  $M$ . As a result, the optimization can be completed very quickly. Moreover, since Problem (8) is convex with respect to  $\mathbf{W}^{t-1}$  for one layer, we do not need to consider all the data for optimization. To make a trade-off between the efficiency and performance, we sample a subset of images randomly from the training data for optimization.<sup>3</sup> Last, since we use SGD to update  $\mathbf{W}_{\mathcal{A}_t}^{t-1}$ , the learning rate  $\gamma$  should be carefully adjusted to achieve an accurate solution.

### F. Stopping conditions

Given a predefined hyperparameter  $\kappa_c^l$  in Problem (7), Algorithm 2 will be stopped if  $\|\mathbf{W}^t\|_{2,0} > \kappa_c^l$ . However,  $\kappa_c^l$  is hard to be determined in practice. To solve this issue, we adopt the following two stopping conditions to terminate Algorithm 2.

**Stopping condition 1:** Since  $\mathcal{L}$  is convex,  $\mathcal{L}(\mathbf{W}^t)$  will monotonically decrease with the iteration index  $t$  in Algorithm 2. Therefore, we can adopt the following stopping condition:

$$\frac{|\mathcal{L}(\mathbf{W}^{t-1}) - \mathcal{L}(\mathbf{W}^t)|}{\mathcal{L}(\mathbf{W}^0)} \leq \epsilon, \quad (10)$$

where  $\epsilon$  is a tolerance value.

**stopping condition 2:** Directly using stopping condition 1 can automatically determine the number of selected channels. However, it may select too many channels for some layers, which introduces extra parameters and computational cost. To solve this issue, we further introduce a channel constraint into stopping condition 1. If the number of selected channels is greater than a predefined value, we stop the algorithm earlier. Specifically, given a minimum pruning rate  $\eta_{\min}$ , we adopt the following stopping condition:

$$\frac{|\mathcal{L}(\mathbf{W}^{t-1}) - \mathcal{L}(\mathbf{W}^t)|}{\mathcal{L}(\mathbf{W}^0)} \leq \epsilon, \quad (11)$$

or  $\|\mathbf{W}^t\|_{2,0} > [(1 - \eta_{\min})c]$ .

If the above condition is achieved, the algorithm is stopped, and the number of selected channels will be automatically determined, i.e.,  $\|\mathbf{W}^t\|_{2,0}$ . The comparisons of different stopping conditions are shown in Section VI-F.

### G. Efficient techniques for implementations

For model compression methods, training cost has always been a key factor in real-world applications. Regarding this issue, we propose two methods to improve the training efficiency of DCP.

**Single round fine-tuning.** In Algorithm 1, fine-tuning plays a crucial role in improving the discriminative power of the intermediate layers. However, it leads to high computational cost. In our conference version [90], we perform fine-tuning and channel selection stage-wisely. In total, we fine-tune the

<sup>3</sup>We study the effect of the number of samples in Section VI-I.

network with  $P + 1$  times, which increases the computational cost of channel pruning. To improve the efficiency of channel pruning, we fine-tune the network with only once in step 3 of Algorithm 1, which reduces the times of fine-tuning. Moreover, the process of the fine-tuning is the same for the network with the same architecture but different pruning rates (e.g., ResNet-18 with 30% pruning rate and ResNet-18 with 50% pruning rate). Therefore, we can store the model after fine-tuning. In this way, the pruned networks with the same architecture but different pruning rates can skip fine-tuning in step 3 of Algorithm 1, which greatly reduces the computational cost of channel pruning. An empirical study on the effect of single round fine-tuning is put in Section VI-C1.

**Feature reusing.** In Algorithm 2, we need to compute the input feature maps of layer  $l$  to compute the loss function. To obtain the input feature maps, we have to feed  $N$  images into the network from layer 1 to layer  $l - 1$ . In [90], this process is repeated for each iteration, which incurs high computational overhead. Since we do not change the input feature maps during channel selection, we can store and reuse the input feature maps once it has been computed. In this way, we can avoid the repeated calculation of the input feature maps, which greatly reduces the computational cost of channel selection. An empirical study on the effect of feature reusing can be found in Section VI-C2.

#### IV. DISCRIMINATION-AWARE KERNEL PRUNING

The proposed DCP can select the channels that really contribute to the discriminative power of the network. However, there exists one limitation. Channel pruning assumes that all kernels in a channel are equally important, which may hamper the performance of the pruned model. In fact, some kernels may not contribute to the discriminative power of the network, resulting in performance degradation of the pruned model.

To solve this issue, we propose a kernel pruning method called discrimination-aware kernel pruning (DKP) to further compress deep networks by removing redundant kernels. Similar to DCP, we introduce a variant of the  $\ell_{2,0}$ -norm constraint on  $\mathbf{W}$  to conduct kernel pruning:

$$\|\mathbf{W}\|_{2,0}^{ker} = \sum_{j=1}^n \sum_{k=1}^c \Omega(\|\mathbf{W}_{j,k,:}\|_F) \leq \kappa_{ker}^l, \quad (12)$$

where  $\kappa_{ker}^l$  is the desired number of kernels at layer  $l$ . When some kernels are removed, the corresponding computation cost w.r.t. the kernels can be effectively reduced.

Starting from a pre-trained model, DKP introduces  $P$  additional losses  $\{\mathcal{L}_S^p\}_{p=1}^P$  evenly to the intermediate layers. Then, DKP fine-tunes the model using the addition losses  $\{\mathcal{L}_S^p\}_{p=1}^P$  and the final loss  $\mathcal{L}_f$  to improve the discriminative power of the intermediate layers. After fine-tuning, DKP conducts kernel selection in a stage-wise manner using a proper discrimination-aware loss and the reconstruction error.

As with DCP, we introduce a variant of  $\ell_{2,0}$ -norm constraint into the loss function in Eq. (6). Thus, the optimization problem for DKP can be formulated as:

$$\min_{\mathbf{W}} \mathcal{L}(\mathbf{W}), \quad \text{s.t.} \quad \|\mathbf{W}\|_{2,0}^{ker} \leq \kappa_{ker}^l. \quad (13)$$

To solve Problem (13), we propose a greedy algorithm for kernel selection similar to Algorithm 2. Instead of choosing

the channels, we choose  $B$  kernels corresponding to the  $B$  largest  $\|\mathbf{G}_{j,k}^{t-1}\|_F = \partial\mathcal{L}/\partial\mathbf{W}_{j,k}^{t-1}$  and put their indices into  $\mathcal{J}_t$ . Then, we update  $\mathcal{A}_t$  by  $\mathcal{A}_t = \mathcal{A}_{t-1} \cup \mathcal{J}_t$ . Once  $\mathcal{A}_t$  is determined, we optimize  $\mathbf{W}^{t-1}$  w.r.t. the selected kernels by minimizing Subproblem (8), which is similar to DCP.

**Relationship with DCP.** Compared with DCP, DKP performs model compression in a finer manner. DKP uses the same algorithm as DCP except that DKP focuses on selecting kernels instead of channels to further compress deep networks at the kernel level.

#### V. EXPERIMENTS

To demonstrate the effectiveness of the proposed method, we apply DCP to various architectures, such as ResNet [23], MobileNetV1 [28] and MobileNetV2 [60], etc. We conduct experiments on both image classification and face recognition. In order to verify the effectiveness of DKP, we apply DKP to ResNet [23] and VGGNet [64]. All implementations are based on PyTorch [57].

We organize the experiments as follows. First, we evaluate the proposed DCP on image classification in Section V-A. Second, we apply DCP to face recognition in Section V-B. Last, we evaluate the proposed DKP in Section V-C.

##### A. Experiments on image classification

1) *Compared methods:* To investigate the effectiveness of the proposed method, we include following methods for study: **DCP:** The proposed channel pruning method with a pre-defined pruning rate  $\eta$ . **Adapt-DCP:** DCP with adaptive stopping condition 2 in Section III-F. **WM:** We shrink the width of a network by a fixed ratio and train it from scratch, which is known as the width-multiplier [28]. **WM+:** Based on WM, we evenly insert additional losses to the network and train it from scratch. **Random-DCP:** Relying on DCP, we randomly choose channels instead of using the gradient-based strategy in Algorithm 2.

We also consider several state-of-the-art channel pruning methods for comparison. On CIFAR-10, we compare DCP with NISP [81], ThiNet [51], CP [27], AMC [25], SFP [24], FPGM [26], PREC [41], Network Slimming [47], NRE [34], and DR [87]. On ILSVRC-12, we compare DCP with SFP [24], SPP [75], CP [27], GDP [43], FPGM [26], ThiNet [51], SSR-L2 [42], AMC [25], and MetaPruning [48].

2) *Data sets and implementation details:* We evaluate the proposed DCP on two image classification data sets, including CIFAR-10 [37] and ILSVRC-12 [8]. CIFAR-10 consists of 50k training samples and 10k testing images with 10 classes. ILSVRC-12 contains 1.28 million training samples and 50k testing images for 1000 classes.

Based on the pre-trained model, we apply our method to select informative channels. We first introduce additional losses to increase the discriminative power of the intermediate layers. In practice, we decide the number of additional losses according to the depth of the network (See Section VI-H).

Specifically, we insert 3 additional losses to ResNet-50 and ResNet-56, and 2 additional losses to VGGNet, ResNet-18, MobileNetV1, and MobileNetV2. Then, we fine-tune the model

TABLE I

PERFORMANCE COMPARISONS ON CIFAR-10. "-" DENOTES THAT THE RESULTS ARE NOT REPORTED. TOP-1 ERR.  $\uparrow$  IS THE TOP-1 ERROR GAP BETWEEN THE PRUNED MODEL AND THE BASELINE MODEL.

Model	Method	Baseline	Pruned	Top-1	#Param. $\downarrow$ (%)	#FLOPs $\downarrow$ (%)
		Top-1 Err. (%)	Top-1 Err. (%)	Err. $\uparrow$ (%)		
ResNet-56	NISP [81]	-	-	+0.03	42.60	43.61
	ThiNet [51]	6.20	7.02	+0.82	49.67	49.78
	CP [27]	7.20	8.20	+1.00	-	50.00
	AMC [25]	7.20	8.10	+0.90	-	50.00
	SFP [24]	6.41	6.65	+0.24	-	52.60
	FPGM [26]	6.41	6.51	+0.10	-	52.60
	WM* [28]	6.26	6.76	+0.50	49.67	49.78
	WM+	6.26	6.65	+0.39	49.67	49.78
	Random-DCP	6.26	6.66	+0.40	49.67	49.78
	DCP	6.26	6.28	+0.02	49.67	49.78
Adapt-DCP	6.26	<b>6.23</b>	<b>-0.03</b>	<b>68.48</b>	<b>54.80</b>	
VGGNet	PFEC [41]	6.75	6.60	-0.15	64.00	34.18
	ThiNet [51]	6.01	6.15	+0.14	48.29	50.08
	CP [27]	6.01	6.33	+0.32	48.29	50.08
	Network Slimming [47]	6.34	6.20	-0.14	88.52	50.94
	NRE [34]	6.54	6.60	+0.06	92.70	67.60
	DR [87]	6.42	6.69	+0.27	88.30	68.63
	WM* [28]	6.02	6.39	+0.37	48.29	50.08
	WM+	6.02	6.12	+0.10	48.29	50.08
	Random-DCP	6.02	5.99	-0.03	48.29	50.08
	DCP	6.02	5.71	-0.31	48.29	50.08
Adapt-DCP	6.02	<b>5.45</b>	<b>-0.57</b>	<b>91.69</b>	<b>69.81</b>	
MobileNetV1	WM* [28]	6.04	6.39	+0.35	43.41	48.63
	WM+	6.04	6.35	+0.31	43.41	48.63
	Random-DCP	6.04	6.36	+0.32	43.41	48.63
	DCP	6.04	5.54	-0.50	43.41	48.63
	Adapt-DCP	6.04	<b>5.43</b>	<b>-0.61</b>	<b>78.26</b>	<b>66.12</b>
MobileNetV2	WM* [28]	5.53	5.98	+0.45	23.59	27.07
	WM+	5.53	5.93	+0.40	23.59	27.07
	Random-DCP	5.53	5.96	+0.42	23.59	27.07
	DCP	5.53	5.37	-0.16	23.59	27.07
	Adapt-DCP	5.53	<b>5.28</b>	<b>-0.25</b>	<b>40.06</b>	<b>34.44</b>

\* The results were obtained by our implementations.

with both the additional losses and the final loss. On CIFAR-10, we fine-tune 100 epochs using a mini-batch size of 128. The learning rate starts from 0.1 and is divided by 10 at epoch 40 and 60. On ILSVRC-12, we fine-tune 60 epochs using a mini-batch size of 256. The learning rate is initialized to 0.01 and divided by 10 at epoch 36, 48, and 54.

After fine-tuning, we conduct channel selection in a stage-wise manner by considering the corresponding additional loss and the reconstruction error of the feature maps. For ResNet-56 and ResNet-50, we set the  $\eta$  and  $\eta_{min}$  to 0.5 and 0.4, respectively. For VGGNet, MobileNetV1 and MobileNetV2,  $\eta$  and  $\eta_{min}$  are set to 0.3 and 0.2, respectively. In our experiment,  $\lambda$  and  $B$  are set to 1.0 and 2.0, respectively.

After channel selection, we fine-tune the whole network with the selected channels only. We use SGD with nesterov [56] for optimization. The momentum and weight decay are set to 0.9 and  $1 \times 10^{-4}$ , respectively. On CIFAR-10, we fine-tune 400 epochs using a mini-batch size of 128. The learning rate is initialized to 0.1 and divided by 10 at epoch 160 and 240. For ResNet-18 and ResNet-50 on ILSVRC-12, we fine-tune the network for 60 epochs with a mini-batch size of 256. The learning rate starts at 0.01 and is divided by 10 at epoch 36,

48 and 54. For MobileNetV1, MobileNetV2 on ILSVRC-12, we fine-tune for 150 epochs and 250 epochs with a mini-batch size of 256. Following [28], [60], we set the weight decay to  $4 \times 10^{-5}$ . The learning rate is initialized to 0.09 and decreased to 0 following the cosine function [50].

3) *Comparisons on CIFAR-10:* We apply DCP to ResNet-56, VGGNet, MobileNetV1, and MobileNetV2 and compare the performance on CIFAR-10. We report the results in Table I.

From Table I, we have following observations. First, the models pruned by DCP significantly outperform the ones pruned by Random-DCP. For example, on VGGNet, DCP reduces the error by 0.28% compared with Random-DCP, which implies the effectiveness of the proposed channel selection strategy. Second, the inserted additional losses improve the performance of the networks. Specifically, WM+ of VGGNet achieves better performance than WM. Third, our proposed DCP shows much better performance than WM+. For example, on VGGNet, DCP outperforms WM+ by **0.41%** on the testing accuracy. Fourth, compared with DCP, Adapt-DCP further improves the performance of the pruned model with much fewer parameters and FLOPs. Specifically, when applying Adapt-DCP on VGGNet, the pruned model with 91.69% and

TABLE II

PERFORMANCE COMPARISONS ON ILSVRC-12. "-" DENOTES THAT THE RESULTS ARE NOT REPORTED. "TOP-1 ERR.  $\uparrow$ " AND "TOP-5 ERR.  $\uparrow$ " DENOTE THE TOP-1 AND TOP-5 ERROR GAP BETWEEN THE PRUNED MODEL AND THE BASELINE MODEL.

Model	Method	Baseline	Pruned	Top-1	Baseline	Pruned	Top-5	#Param. $\downarrow$ (%)	#FLOPs $\downarrow$ (%)
		Top-1 Err. (%)	Top-1 Err. (%)	Err. $\uparrow$ (%)	Top-5 Err. (%)	Top-5 Err. (%)	Err. $\uparrow$ (%)		
ResNet-50	SFP [24]	23.85	25.39	+1.54	7.13	7.94	+0.81	-	41.80
	GAL [44]	23.85	28.05	+4.20	7.13	9.06	+1.93	16.86	43.03
	Taylor-FO-BN [52]	23.82	25.50	+1.68	-	-	-	44.53	44.99
	SPP [75]	-	-	-	8.80	9.60	+0.80	-	50.00
	CP [27]	-	-	-	7.80	9.20	+1.40	-	50.00
	GDP [43]	24.87	28.11	+3.24	7.70	9.29	+1.59	-	51.30
	FPGM [26]	23.85	25.17	+1.32	7.13	7.68	+0.55	-	53.50
	ThiNet [51]	24.70	27.97	+3.27	7.80	9.01	+1.21	51.55	55.50
	SSR-L2 [42]	24.88	28.53	+3.65	7.70	9.81	+2.11	52.94	56.41
	WM* [28]	23.99	26.47	+2.48	7.07	8.52	+1.45	51.55	55.50
	WM*(Scratch-B) [49]	23.99	25.44	+1.45	7.07	8.03	+0.96	51.55	55.50
DCP	23.99	25.01	+1.02	7.07	7.80	+0.73	51.55	<b>55.50</b>	
Adapt-DCP	23.99	<b>24.85</b>	<b>+0.86</b>	7.07	<b>7.70</b>	<b>+0.63</b>	<b>54.99</b>	52.41	
MobileNetV1	NetAdapt [78]	29.10	30.90	+1.80	-	-	-	-	12.63
	AMC [25]	29.10	29.51	+0.41	10.10	10.69	+0.59	43.09	48.42
	MetaPruning [48]	29.10	29.60	+0.50	-	-	-	-	50.62
	WM [28]	29.10	31.60	+2.50	10.10	11.80	+1.70	38.90	42.86
	DCP	29.12	29.52	+0.40	10.22	<b>10.61</b>	<b>+0.39</b>	<b>45.47</b>	49.67
	Adapt-DCP	29.12	<b>29.50</b>	<b>+0.38</b>	10.22	10.78	+0.56	43.27	<b>51.25</b>
MobileNetV2	AMC [25]	28.20	29.15	+0.95	9.00	10.09	+1.09	33.51	30.06
	MetaPruning [48]	28.20	28.80	+0.60	-	-	-	-	27.67
	WM [60]	28.20	30.20	+2.00	9.00	10.40	+1.40	25.02	40.52
	DCP	28.12	28.79	+0.67	9.70	10.01	+0.31	34.24	<b>32.21</b>
	Adapt-DCP	28.12	<b>28.55</b>	<b>+0.43</b>	9.70	<b>9.94</b>	<b>+0.24</b>	<b>35.87</b>	31.08

\* The results were obtained by our implementations.

TABLE III

INFERENCE ACCELERATION OF THE PRUNED MODELS ON ILSVRC-12. WE REPORT THE FORWARD TIME TESTED ON A MOBILE CPU (QUALCOMM SNAPDRAGON 845).

Network	$\eta$	#Param. (M)	#FLOPs (M)	Mobile CPU	Speedup
				Time (ms)	Ratio
MobileNetV1	0.00	4.23	11.32	107.25	1.00
	0.30	<b>2.31</b>	<b>5.70</b>	<b>55.65</b>	<b>1.93</b>
MobileNetV2	0.00	3.50	5.95	62.88	1.00
	0.30	<b>2.30</b>	<b>4.03</b>	<b>44.25</b>	<b>1.42</b>

69.81% reductions in parameters and FLOPs even lowers the testing error by 0.26% compared with DCP.

Compared with several state-of-the-art methods, our method achieves the best performance. For example, ThiNet [51] prunes VGGNet by 48.29% of the parameters and 50.08% of the FLOPs with a 0.14% accuracy drop, but our proposed DCP achieves the same speedup ratio with a **0.31%** improvement in accuracy. Moreover, for VGGNet, Adapt-DCP outperforms NRE [34] and DR [87] and obtains a **91.69%** reduction in the model size and **69.81%** in FLOPs. These results justify the superior performance of our proposed DCP and Adapt-DCP.

4) *Comparisons on ILSVRC-12*: To verify the effectiveness of the proposed method on the large-scale data set, we evaluate our method on ILSVRC-12 and report the Top-1 and Top-5 error with single view evaluation in Table II. We first apply DCP to compress ResNet-50. Compared with WM (Scratch-B) [49], which leads to 1.45% increase on the Top-1 error, DCP only results in **1.02%** degradation on the Top-1 accuracy,

which demonstrates the effectiveness of DCP. Compared with FPGM [26], DCP achieves 0.30% improvement on the Top-1 accuracy with 55.50% reduction in FLOPs. More critically, the model pruned by Adapt-DCP with the smaller model size even outperforms DCP by 0.16% and 0.10% on Top-1 and Top-5 accuracy, respectively.

Apart from ResNet-50, we also apply DCP to compact and efficient neural networks, such as MobileNetV1 [28] and MobileNetV2 [60]. Compared with AMC [25] and MetaPruning [48], our proposed DCP achieves better performance. For example, on MobileNetV2, DCP outperforms AMC [25] by 0.28% and 0.78% on the Top-1 and Top-5 accuracy, respectively. Moreover, with Adapt-DCP, our pruned MobileNetV2 with greater reduction in FLOPs outperforms MetaPruning [48] by 0.17% on the Top-1 accuracy. These results demonstrate the effectiveness of DCP and Adapt-DCP.

5) *Inference acceleration on mobilephone*: We further investigate the inference acceleration of the pruned model with DCP on a mobile phone. We perform the evaluations on a Xiaomi 8 smartphone, which is equipped with a 2.8 GHz Qualcomm Snapdragon 845 mobile processor. The test-phase computation is carried out on a single large CPU core without GPU acceleration. We report the results on ILSVRC-12 in Table III.

Compared with the pre-trained model, MobileNetV1 with the pruning rate of 30% achieves nearly  $2\times$  acceleration on the mobile phone. Moreover, the execution of our pruned MobileNetV2 only requires 44.25ms, which matches the requirements for mobile and embedded vision applications.

TABLE IV

PERFORMANCE COMPARISON OF DIFFERENT METHODS ON FACE RECOGNITION. “VR” REFERS TO VERIFICATION TAR (TRUE ACCEPTED RATE) AND “FAR10<sup>-6</sup>” REFERS TO THE FALSE ACCEPTED RATE AT 10<sup>-6</sup>. WE DO NOT REPORT THE INFERENCE TIME OF SPHEREFACE AND COSFACE DUE TO ITS LARGE MODEL SIZE AND COMPUTATIONAL COSTS.

Model	Validation Accuracy (%)			VR@FAR10 <sup>-6</sup> (%)	#Param. (M)	#FLOPs (G)	Mobile CPU Times (ms)	Speedup Ratio
	LFW	CFP-FP	AgeDB-30	MegaFace				
SphereFace [61]	99.76	93.70	97.56	97.43	65.16	24.17	-	-
CosFace [74]	99.80	94.40	97.91	98.36	65.16	24.17	-	-
LResNet34E-IR [10]	99.72	96.39	98.03	96.71	31.81	7.10	391.52	1.00
LResNet34E-IR (prune 25% channels)	99.70	<b>96.71</b>	97.63	<b>97.03</b>	27.12	5.35	308.72	1.27
LResNet34E-IR (prune 50% channels)	99.70	95.90	97.70	96.14	<b>22.42</b>	<b>3.60</b>	<b>232.61</b>	<b>1.68</b>
MobileFaceNet [6]	99.50	92.23	95.63	90.38	1.00	0.44	36.90	1.00
MobileFaceNet (prune 25% channels)	99.38	92.17	95.47	90.33	<b>0.79</b>	<b>0.33</b>	<b>28.71</b>	<b>1.29</b>

TABLE V

PRUNING RESULTS OF DKP ON ILSVRC-12. THE TOP-1 AND TOP-5 ERROR (%) OF THE PRE-TRAINED RESNET-18 ARE 30.36 AND 11.02, RESPECTIVELY.

Model	Method	Pruned	Top-1	Pruned	Top-5	#Param. ↓ (%)	#FLOPs ↓ (%)
		Top-1 Err. (%)	Err. ↑ (%)	Top-5 Err. (%)	Err. ↑ (%)		
ResNet-18	DCP	32.64	+2.28	12.38	+1.36	47.00	46.22
	DKP	<b>32.57</b>	<b>+2.21</b>	<b>12.20</b>	<b>+1.18</b>	<b>47.31</b>	<b>46.40</b>
	DCP	35.89	+5.53	<b>14.22</b>	<b>+3.20</b>	65.70	64.25
	DKP	<b>35.54</b>	<b>+5.18</b>	14.26	+3.24	<b>65.89</b>	<b>64.77</b>

TABLE VI

PRUNING RESULTS OF DKP ON CIFAR-10. THE TOP-1 ERROR (%) OF THE PRE-TRAINED RESNET-56 AND VGGNET ARE 6.26 AND 6.02, RESPECTIVELY.

Model	Method	Pruned	Top-1	#Param. ↓ (%)	#FLOPs ↓ (%)
		Top-1 Err. (%)	Err. ↑ (%)		
ResNet-56	DCP	6.28	+0.02	49.67	49.78
	DKP	<b>6.23</b>	<b>-0.03</b>	<b>51.53</b>	<b>50.59</b>
	DCP	7.02	+0.76	68.29	68.44
	DKP	<b>6.96</b>	<b>+0.70</b>	<b>68.62</b>	<b>68.84</b>
VGGNet	DCP	6.24	+0.22	72.01	<b>74.30</b>
	DKP	<b>6.17</b>	<b>+0.15</b>	<b>73.16</b>	<b>74.26</b>
	DCP	7.98	+1.96	88.42	90.24
	DKP	<b>7.74</b>	<b>+1.72</b>	<b>89.39</b>	<b>90.42</b>

## B. Experiments on Face Recognition

1) *Compared methods*: We apply the proposed DCP to LResNet34E-IR [10] and MobileFaceNet [6] on face recognition. To evaluate the proposed DCP method, we consider several face recognition models for comparison, including SphereFace [46] and CosFace [74].

2) *Data sets and implementation details*: We evaluate the proposed DCP method on four benchmark data sets, including LFW [30], CFP-FP [62], AgeDB-30 [54], and MegaFace [36].

LFW [30] contains 13,233 face images from 5,749 identities. CFP [62] consists of 500 identities, each with 10 frontal and 4 profile images. AgeDB-30 [54] contains 12,240 images of 440 identities. MegaFace [36] is a very challenging benchmark data set to evaluate the performance of face recognition methods at a scale of million distractors.

We use the refined MS-Celeb-1M [19] released by [9] for training. The training data set consists of 5.8M face images from 85k individuals. With the same settings in [9], we first train LResNet34E-IR [10] and MobileFaceNet [6] from scratch. Then, we adopt our proposed DCP to compress the pre-trained

models.

Before channel pruning, we first insert 2 additive angular margin losses [9] to LResNet34E-IR and MobileFaceNet. Then, we fine-tune 15 epochs with both the discrimination-aware losses and the final loss. We use SGD with a mini-batch size of 512. The learning rate is initialized to 0.01 and divided by 10 at epoch 4, 8, and 12.

After fine-tuning, we perform channel selection to select the informative channels. After channel selection, we fine-tune the whole network for 28 epochs. The learning rate is initialized to 0.01 and divided by 10 at epoch 8, 16 and 24. We use SGD with mini-batch size of 512.

3) *Performance comparison*: We report the results in Table IV. From the results, we observe that the pruned model with small pruning rates achieve nearly the same performance to the pre-trained model. For example, for LResNet34E-IR, the pruned model with the pruning rate of 25% even outperforms the pre-trained model on CFP-FP and MegaFace. Moreover, for MobileFaceNet, the pruned model achieves comparable performance as the pre-trained model with only 0.79M parameters and 28.71ms for inference, which is suitable for resource-limited devices.

Compared with SphereFace [61] and CosFace [74], our pruned LResNet34E-IR achieves comparable performance with much smaller number of parameters and FLOPs. Even with the pruning rate of 50%, our pruned LResNet34E-IR still achieves comparable performance to the pre-trained model. These results demonstrate the effectiveness of the proposed DCP on face recognition.

## C. Effectiveness of DKP

1) *Compared methods*: To investigate the effectiveness of DKP, we include the following methods for study. **DCP**: The proposed channel pruning method with a fixed pruning rate.

TABLE VII

COMPARISONS ON RESNET-18 AND RESNET-50 WITH DIFFERENT PRUNING RATES. WE REPORT THE TOP-1 AND TOP-5 ERROR (%) ON ILSVRC-12.

Network	$\eta$	Top-1	Top5	#Param.	#FLOPs
		Err. $\uparrow$ (%)	Err. $\uparrow$ (%)	$\downarrow$ (%)	$\downarrow$ (%)
ResNet-18	0%	30.36	11.02	-	-
	30%	<b>30.77</b>	<b>11.03</b>	28.05	27.49
	50%	32.64	12.38	47.01	46.22
	70%	35.89	14.22	<b>65.70</b>	<b>64.25</b>
ResNet-50	0%	23.99	7.07	-	-
	30%	<b>23.63</b>	<b>6.96</b>	33.40	35.72
	50%	25.01	7.80	51.55	55.50
	70%	27.28	8.83	<b>65.90</b>	<b>71.09</b>

**DKP**: The proposed kernel pruning method with a fixed pruning rate.

2) *Data sets and implementation details*: We evaluate the performance of the pruned model on CIFAR-10 and ILSVRC-12. For kernel selection, we use the same additional losses introduced in DCP. After kernel selection, we fine-tune the whole network with the selected kernels only.

3) *Performance comparison*: After channel selection, we further apply DKP to ResNet-56, VGGNet and ResNet-18. We report the results in Table V and Table VI. From the results, the models pruned by DKP with greater reductions in parameters and FLOPs outperform the models obtained by DCP. For example, for ResNet-18, DKP outperforms DCP by 0.17% on the Top-1 accuracy with 47.17% and 46.56% reductions in the parameters and FLOPs. These results demonstrate the effectiveness of DKP. Moreover, the performance improvement of DKP built on DCP goes better with the increase of pruning rate. To be specific, the model pruned by DKP with 47.31% reduction in parameters only achieves 0.07% improvement over DCP. Nevertheless, the model pruned by DKP with 65.89% reduction in parameters reduces the Top-1 error by 0.35% compared with the one pruned by DCP.

## VI. ABLATION STUDIES

In this section, we conduct ablation studies for the proposed DCP. 1) We investigate the effect of using different pruning rates in Section VI-A. 2) We explore the effect of using different  $\lambda$  in Section VI-B. 3) We explore the effect of efficient training strategies in Section VI-C. 4) We explore the effect of  $B$  in Section VI-D. 5) We compare different stopping conditions in Section VI-F. 6) We discuss the effect of the tolerance  $\epsilon$  in the stopping conditions in Section VI-E. 7) We visualize the feature maps w.r.t. the pruned/selected channels of ResNet-18 and MobileNetV2 in Section VI-G. 8) We explore the influence of the number of additional losses in Section VI-H. 9) We explore the effect of the number of samples in channel selection in Section VI-I.

### A. Performance with different pruning rates

To study the effect of using different pruning rates  $\eta$ , we prune 30%, 50%, and 70% channels from ResNet-18 and ResNet-50, and evaluate the pruned models on ILSVRC-12. The experimental results are shown in Table VII.

TABLE VIII

PRUNING RESULTS OF RESNET-56 AND MOBILENETV1 WITH DIFFERENT  $\lambda$ . WE REPORT THE TESTING ERROR (%) ON CIFAR-10.

$\lambda$	0	0.1	0.5	1	$1(\mathcal{L}_M \text{ only})$	5	10
ResNet-56	5.94	5.96	5.87	<b>5.80</b>	5.99	5.85	5.93
MobileNetV1	5.66	5.46	5.59	5.54	5.43	<b>5.42</b>	5.56

TABLE IX

EFFECT OF EFFICIENT SINGLE ROUND FINE-TUNING. WE REPORT THE TESTING ERROR (%) AND THE TIME OF CHANNEL PRUNING ON CIFAR-10 AND ILSVRC-12.

Model	Method	Top-1	Top-5	Time (hour)
		Err. $\uparrow$ (%)	Err. $\uparrow$ (%)	
ResNet-56 (CIFAR-10)	DCP [90]	6.51	-	7.58
	DCP	<b>6.26</b>	-	<b>2.83</b>
ResNet-18 (ILSVRC-12)	DCP [90]	<b>35.88</b>	<b>14.32</b>	31.78
	DCP	35.89	14.34	<b>5.18</b>

In general, the pruned models perform worse with the increase of the pruning rate. However, our pruned ResNet-50 with a pruning rate of 30% outperforms the pre-trained model with **0.36%** and **0.11%** improvement on the Top-1 and Top-5 accuracy, respectively. Additionally, the performance degradation of ResNet-50 is smaller than that of ResNet-18 with the same pruning rate. For example, when pruning 50% of the channels, it only leads to 1.02% increase on the Top-1 error for ResNet-50. In contrast, it results in 2.28% increase of the Top-1 error for ResNet-18. It can be attributed to that, compared with ResNet-18, ResNet-50 is more redundant with more parameters, thus it is easier to be pruned.

### B. Effect of the trade-off hyperparameter $\lambda$

We prune 30% channels of ResNet-56 and MobileNetV1 on CIFAR-10 with different  $\lambda$  values. We report the testing error in Table VIII. From the table, the performance of the pruned model first improves and then degrades with the increasing  $\lambda$ . Here, a larger  $\lambda$  implies that more emphasis is placed on the reconstruction error (See Eq. (6)). This demonstrates the effectiveness of the discrimination-aware strategy for channel selection. It is worth mentioning that both the reconstruction error and the cross-entropy loss contribute to better performance of the pruned model, which strongly supports the motivation to select the important channels by  $\mathcal{L}_S^p$  and  $\mathcal{L}_M$ . Note that setting  $\lambda$  to 1.0 does not lead to the best performance considering different architectures and data sets. For simplicity, we set  $\lambda$  to 1.0 by default in our experiments.

### C. Effect of the improved training techniques

1) *Effect of the single round fine-tuning*: To evaluate the effectiveness of the single round fine-tuning, we prune 50% channels of ResNet-56 on CIFAR-10 and 70% channels of ResNet-18 on ILSVRC-12. We compare the proposed DCP with the conference version [90] and report the testing error and time of channel pruning in Table IX. From the table, the proposed DCP with single round fine-tuning significantly reduces the training time while maintaining comparable performance to

TABLE X

EFFECT OF FEATURE REUSING. WE PRUNE 50% CHANNELS FROM RESNET-56 AND REPORT THE TESTING ERROR (%) AND THE TIME OF CHANNEL PRUNING ON CIFAR-10.

Model	Testint Err. (%)	Time (hour)
w/o feature reusing	<b>6.26</b>	2.83
w/ feature reusing	6.28	<b>1.85</b>

TABLE XI

PRUNING RESULTS OF RESNET-56 WITH DIFFERENT  $B$ . WE REPORT THE TESTING ERROR (%) AND THE TIME OF CHANNEL PRUNING ON CIFAR-10.

$B$	Testing Err. (%)	Time (hour)
1	<b>6.22</b>	1.85
2	6.28	0.90
4	6.32	<b>0.48</b>

TABLE XII

EFFECT OF  $\epsilon$  FOR CHANNEL SELECTION. WE PRUNE VGGNET WITH DIFFERENT STOPPING CONDITIONS AND REPORT THE TESTING ERROR (%) ON CIFAR-10.

Model	$\epsilon$	Top-1 Err. (%)	#Param. ↓ (%)	#FLOPs ↓ (%)
w/ stopping condition 1	$5 \times 10^{-4}$	6.29	<b>96.16</b>	<b>67.87</b>
	$3 \times 10^{-4}$	5.91	94.59	56.73
	$1 \times 10^{-4}$	<b>5.31</b>	90.93	30.80
w/ stopping condition 2	$5 \times 10^{-4}$	6.36	<b>95.95</b>	<b>84.61</b>
	$3 \times 10^{-4}$	5.87	94.74	79.66
	$1 \times 10^{-4}$	<b>5.45</b>	91.69	69.81

the previous DCP [90], which demonstrates the effectiveness and efficiency of the improved fine-tuning strategy.

2) *Effect of the feature reusing*: To study the effect of the feature reusing, we prune 50% channels from ResNet-56 and report the testing error and time of channel pruning in Table X. As shown in the table, pruning with the feature reusing achieves comparable performance to the model without the feature reusing. However, pruning with the feature reusing greatly reduces the time of channel pruning, which demonstrates its effectiveness. Due to the superior performance of the feature reusing, we use it by default in our experiments.

#### D. Effect of the hyperparameter $B$

To evaluate the effect of  $B$ , we prune 50% channels of ResNet-56 on CIFAR-10 with different  $B$  and report the results in Table XI. Here, a larger  $B$  indicates that we select more channels at each iteration in Algorithm 2. As a result, fewer iterations are required. From Table XI, the time of channel pruning decreases with the increasing of  $B$  while the performance of DCP degrades. To make a trade-off between accuracy and complexity, we set  $B$  to 2 in our experiments.

#### E. Effect of the tolerance $\epsilon$ in the stopping condition

We test different tolerance values in Eq. (11). Here, we prune VGGNet on CIFAR-10 with  $\epsilon \in \{1 \times 10^{-4}, 3 \times 10^{-4}, 5 \times 10^{-4}\}$ . We show the experimental results in Table XII. In general, a smaller  $\epsilon$  will lead to a more rigorous stopping condition. Hence, more channels will be selected. As a result, the performance

TABLE XIII

PRUNING RESULTS OF RESNET-56 WITH DIFFERENT STOPPING CONDITIONS. WE REPORT THE TESTING ERROR (%) ON CIFAR-10.

Model	Testing Err. (%)	#Param. ↓ (%)	#FLOPs ↓ (%)
w/ stopping condition 1	6.36	65.20	46.82
w/ stopping condition 2	<b>6.23</b>	<b>68.48</b>	<b>54.80</b>

TABLE XIV

EFFECT OF THE NUMBER OF ADDITIONAL LOSSES. WE PRUNE 50% CHANNELS FROM RESNET-56 AND 30% CHANNELS FROM MOBILENETV1. WE REPORT THE TESTING ERROR ON CIFAR-10. THE TESTING ERROR (%) OF BASELINE RESNET-56 AND MOBILENET V1 ARE 6.26 AND 6.04, RESPECTIVELY.

#Additional Losses	Err. gap (%)	
	ResNet-56	MobileNetV1
1	+0.10	-0.28
3	+0.02	-0.54
5	+0.01	-0.65
7	-0.08	-0.70

of the pruned model is improved with the decreasing of  $\epsilon$ . This experiment demonstrates the effectiveness of the stopping condition for automatically determining the pruning rate.

#### F. Effect of different stopping conditions

To study the effect of different stopping conditions in Section III-F, we prune 50% channels from ResNet-56 using Adapt-DCP with different stopping conditions. We report the results in Table XIII. From the table, pruning with stopping condition 2 achieves better performance with a greater reduction in parameters and FLOPs compared with the one with stopping condition 1. To further explore the effect of different stopping conditions, we visualize the pruned network structure of ResNet-56. From Figure 3, pruning with stopping condition 2 selects fewer channels in shallow layers compared with the one with stopping condition 1. As a result, the pruned models have fewer parameters and lower computational cost. Due to the superior performance of stopping condition 2, we use it by default in our experiments.

#### G. Visualization of feature maps

We further visualize the feature maps w.r.t. the pruned and selected channels of the second block in MobileNetV2 in Figure 2. From the results, the feature maps of the pruned channels are less informative compared with those of the selected ones. It proves that the proposed DCP selects the channels with strong discriminative power for the network.

#### H. Effect of the number of additional losses

To study the effect of the number of additional losses, we prune 50% channels from ResNet-56 and 30% channels from MobileNetV1 on CIFAR-10. As shown in Table XIV, adding more losses results in better performance. For example, ResNet-56 with three additional losses outperforms the one with one additional loss. However, adding too many losses may lead

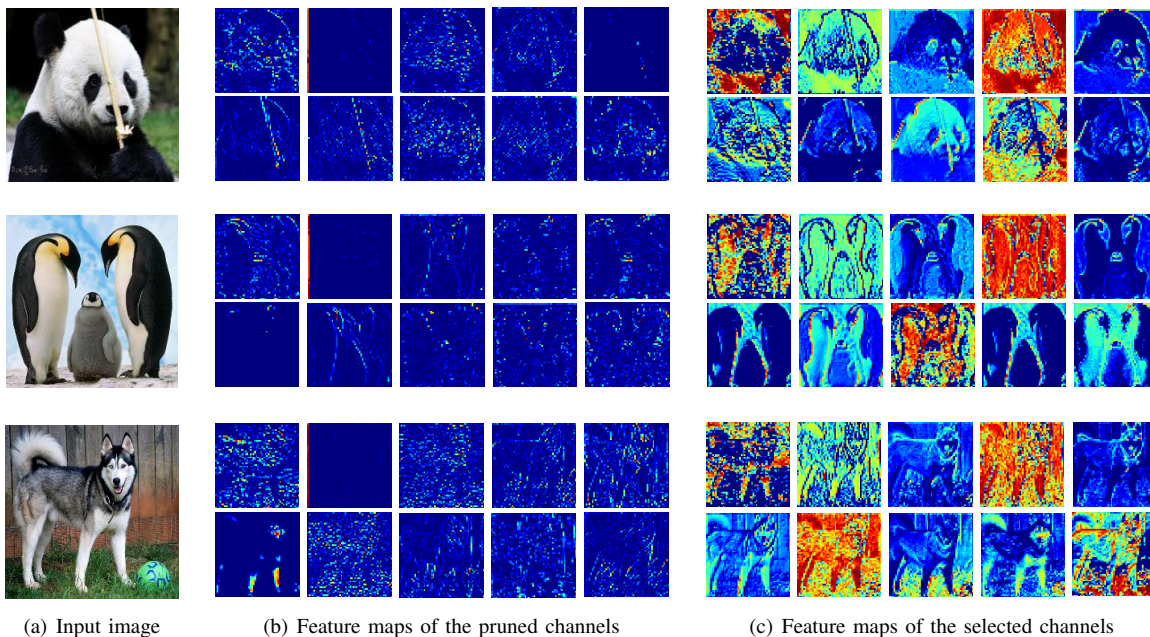


Fig. 2. Visualization of the feature maps of the pruned/selected channels of the second block in MobileNetV2.

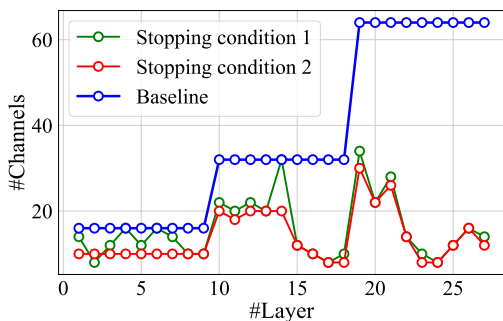


Fig. 3. Visualization of network architecture of the pruned ResNet-56 with different stopping conditions.

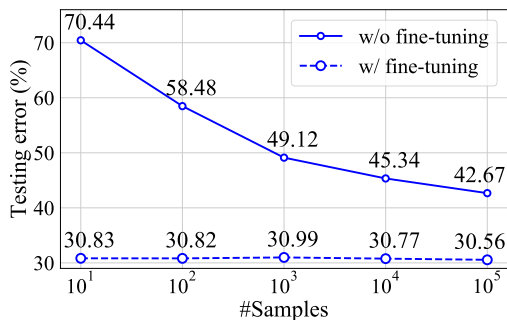


Fig. 4. Effect of the number of samples for channel selection. We prune 30% channels from ResNet-18 and report the Top-1 error with and without fine-tuning on ILSVRC-12.

to a little gain in performance but incur significant increase of the computational cost. Heuristically, we find that adding losses every 5-10 blocks is sufficient to make a good trade-off between accuracy and complexity.

### I. Effect of the number of samples

To study the influence of the number of samples on channel selection, we prune 30% channels from ResNet-18 on ILSVRC-12 with different numbers of samples, *i.e.*, from 10 to 100k. The experimental results are shown in Figure 4.

In general, with more samples for channel selection, the performance degradation of the pruned model can be further reduced. However, it also leads to a more expensive computation cost. Moreover, the performance gap between different numbers of samples becomes smaller after fine-tuning. To make a trade-off between performance and efficiency, we use 10k samples in our experiments for ILSVRC-12. For small data sets such as CIFAR-10, we use the whole training set for channel selection.

## VII. CONCLUSIONS

In this paper, we have proposed a discrimination-aware channel pruning (DCP) method for the compression of deep neural networks. By introducing the additional losses, the discriminative power of intermediate layers can be improved. Then, we perform the channel selection in a stagewise manner. In order to choose channels, we formulate the channel pruning as a sparsity-induced optimization problem and proposed a greedy algorithm to solve it. Based on DCP, we propose several techniques to reduce the computational burden of channel pruning. To reduce kernel level redundancy, we propose a discrimination-aware kernel pruning (DKP) method to further perform model compression in the kernel level. Extensive results on both image classification and face recognition tasks demonstrate the effectiveness of the proposed methods.

## REFERENCES

- [1] J. M. Alvarez and M. Salzmann. Learning the number of neurons in deep networks. In *Advances in Neural Information Processing Systems*, pages 2270–2278, 2016.
- [2] S. Anwar, K. Hwang, and W. Sung. Structured pruning of deep convolutional neural networks. *ACM Journal on Emerging Technologies in Computing Systems*, 13(3):32, 2017.
- [3] S. Bahmani, B. Raj, and P. T. Boufounos. Greedy sparsity-constrained optimization. *Journal of Machine Learning Research*, 14(Mar):807–841, 2013.
- [4] A. Bulat and Y. Tzimiropoulos. Hierarchical binary cnns for landmark localization with limited resources. *IEEE Transactions on Pattern Analysis and Machine Intelligence*, 2018.
- [5] J. Cao, Y. Guo, Q. Wu, C. Shen, J. Huang, and M. Tan. Adversarial learning with local coordinate coding. In *International Conference on Machine Learning*, volume 80, pages 707–715, 2018.
- [6] S. Chen, Y. Liu, X. Gao, and Z. Han. Mobilefacenets: Efficient cnns for accurate real-time face verification on mobile devices. In *Chinese Conference on Biometric Recognition*, pages 428–438. Springer, 2018.
- [7] J. Choi, Z. Wang, S. Venkataramani, P. I.-J. Chuang, V. Srinivasan, and K. Gopalakrishnan. Pact: Parameterized clipping activation for quantized neural networks. *arXiv preprint arXiv:1805.06085*, 2018.
- [8] J. Deng, W. Dong, R. Socher, L.-J. Li, K. Li, and L. Fei-Fei. Imagenet: A large-scale hierarchical image database. In *IEEE Conference on Computer Vision and Pattern Recognition*, pages 248–255, 2009.
- [9] J. Deng, J. Guo, X. Niannan, and S. Zafeiriou. Arcface: Additive angular margin loss for deep face recognition. In *IEEE Conference on Computer Vision and Pattern Recognition*, 2019.
- [10] J. Deng, J. Guo, X. Niannan, and S. Zafeiriou. Arcface: Additive angular margin loss for deep face recognition. In *IEEE Conference on Computer Vision and Pattern Recognition*, pages 4690–4699, 2019.
- [11] E. L. Denton, W. Zaremba, J. Bruna, Y. LeCun, and R. Fergus. Exploiting linear structure within convolutional networks for efficient evaluation. In *Advances in Neural Information Processing Systems*, pages 1269–1277, 2014.
- [12] Y. Gong, L. Liu, M. Yang, and L. Bourdev. Compressing deep convolutional networks using vector quantization. *arXiv preprint arXiv:1412.6115*, 2014.
- [13] I. Goodfellow, J. Pouget-Abadie, M. Mirza, B. Xu, D. Warde-Farley, S. Ozair, A. Courville, and Y. Bengio. Generative adversarial nets. In *Advances in Neural Information Processing Systems*, pages 2672–2680, 2014.
- [14] Y. Guo, Q. Chen, J. Chen, J. Huang, Y. Xu, J. Cao, P. Zhao, and M. Tan. Dual reconstruction nets for image super-resolution with gradient sensitive loss. *arXiv preprint arXiv:1809.07099*, 2018.
- [15] Y. Guo, Q. Chen, J. Chen, Q. Wu, Q. Shi, and M. Tan. Auto-embedding generative adversarial networks for high resolution image synthesis. *IEEE Transactions on Multimedia*, 2019.
- [16] Y. Guo, M. Tan, Q. Wu, J. Chen, A. V. D. Hengel, and Q. Shi. The shallow end: Empowering shallower deep-convolutional networks through auxiliary outputs. *arXiv preprint arXiv:1611.01773*, 2016.
- [17] Y. Guo, Q. Wu, C. Deng, J. Chen, and M. Tan. Double forward propagation for memorized batch normalization. In *AAAI Conference on Artificial Intelligence*, 2018.
- [18] Y. Guo, A. Yao, and Y. Chen. Dynamic network surgery for efficient dnns. In *Advances in Neural Information Processing Systems*, pages 1379–1387, 2016.
- [19] Y. Guo, L. Zhang, Y. Hu, X. He, and J. Gao. Ms-celeb-1m: A dataset and benchmark for large-scale face recognition. In *European Conference on Computer Vision*, pages 87–102. Springer, 2016.
- [20] Y. Guo, Y. Zheng, M. Tan, Q. Chen, J. Chen, P. Zhao, and J. Huang. Nat: Neural architecture transformer for accurate and compact architectures. In *Advances in Neural Information Processing Systems*, pages 735–747. Curran Associates, Inc., 2019.
- [21] S. Han, H. Mao, and W. J. Dally. Deep compression: Compressing deep neural networks with pruning, trained quantization and Huffman coding. In *International Conference on Learning Representations*, 2016.
- [22] S. Han, J. Pool, J. Tran, and W. Dally. Learning both weights and connections for efficient neural network. In *Advances in Neural Information Processing Systems*, pages 1135–1143, 2015.
- [23] K. He, X. Zhang, S. Ren, and J. Sun. Deep residual learning for image recognition. In *IEEE Conference on Computer Vision and Pattern Recognition*, pages 770–778, 2016.
- [24] Y. He, G. Kang, X. Dong, Y. Fu, and Y. Yang. Soft filter pruning for accelerating deep convolutional neural networks. In *International Joint Conferences on Artificial Intelligence*, pages 2234–2240. AAAI Press, 2018.
- [25] Y. He, J. Lin, Z. Liu, H. Wang, L.-J. Li, and S. Han. Amc: Automl for model compression and acceleration on mobile devices. In *European Conference on Computer Vision*, pages 784–800, 2018.
- [26] Y. He, P. Liu, Z. Wang, Z. Hu, and Y. Yang. Filter pruning via geometric median for deep convolutional neural networks acceleration. In *IEEE Conference on Computer Vision and Pattern Recognition*, 2019.
- [27] Y. He, X. Zhang, and J. Sun. Channel pruning for accelerating very deep neural networks. In *IEEE International Conference on Computer Vision*, pages 1389–1397, 2017.
- [28] A. G. Howard, M. Zhu, B. Chen, D. Kalenichenko, W. Wang, T. Weyand, M. Andreetto, and H. Adam. Mobilenets: Efficient convolutional neural networks for mobile vision applications. *arXiv preprint arXiv:1704.04861*, 2017.
- [29] H. Hu, R. Peng, Y.-W. Tai, and C.-K. Tang. Network trimming: A data-driven neuron pruning approach towards efficient deep architectures. *arXiv preprint arXiv:1607.03250*, 2016.
- [30] G. B. Huang, M. Ramesh, T. Berg, and E. Learned-Miller. Labeled faces in the wild: A database for studying face recognition in unconstrained environments. Technical report, Technical Report 07-49, University of Massachusetts, Amherst, 2007.
- [31] I. Hubara, M. Courbariaux, D. Soudry, R. El-Yaniv, and Y. Bengio. Binarized neural networks. In *Advances in Neural Information Processing Systems*, pages 4107–4115, 2016.
- [32] S. Ioffe and C. Szegedy. Batch normalization: Accelerating deep network training by reducing internal covariate shift. In *International Conference on Machine Learning*, pages 448–456, 2015.
- [33] M. Jaderberg, A. Vedaldi, and A. Zisserman. Speeding up convolutional neural networks with low rank expansions. *arXiv preprint arXiv:1405.3866*, 2014.
- [34] C. Jiang, G. Li, C. Qian, and K. Tang. Efficient dnn neuron pruning by minimizing layer-wise nonlinear reconstruction error. In *International Joint Conferences on Artificial Intelligence*, volume 2018, pages 2–2, 2018.
- [35] S. Jung, C. Son, S. Lee, J. Son, J.-J. Han, Y. Kwak, S. J. Hwang, and C. Choi. Learning to quantize deep networks by optimizing quantization intervals with task loss. In *IEEE Conference on Computer Vision and Pattern Recognition*, pages 4350–4359, 2019.
- [36] I. Kemelmacher-Shlizerman, S. M. Seitz, D. Miller, and E. Brossard. The megaface benchmark: 1 million faces for recognition at scale. In *IEEE Conference on Computer Vision and Pattern Recognition*, pages 4873–4882, 2016.
- [37] A. Krizhevsky and G. Hinton. Learning multiple layers of features from tiny images. *Tech Report*, 2009.
- [38] A. Krizhevsky, I. Sutskever, and G. E. Hinton. Imagenet classification with deep convolutional neural networks. In *Advances in Neural Information Processing Systems*, pages 1097–1105, 2012.
- [39] C.-Y. Lee, S. Xie, P. Gallagher, Z. Zhang, and Z. Tu. Deeply-supervised nets. In *International Conference on Artificial Intelligence and Statistics*, pages 562–570, 2015.
- [40] N. Lee, T. Ajanthan, and P. H. Torr. Snip: Single-shot network pruning based on connection sensitivity. In *International Conference on Learning Representations*, 2019.
- [41] H. Li, A. Kadav, I. Durdanovic, H. Samet, and H. P. Graf. Pruning filters for efficient convnets. In *International Conference on Learning Representations*, 2017.
- [42] S. Lin, R. Ji, Y. Li, C. Deng, and X. Li. Toward compact convnets via structure-sparsity regularized filter pruning. *IEEE Transactions on Neural Networks and Learning Systems*, pages 1–15, 2019.
- [43] S. Lin, R. Ji, Y. Li, Y. Wu, F. Huang, and B. Zhang. Accelerating convolutional networks via global & dynamic filter pruning. In *International Joint Conferences on Artificial Intelligence*, pages 2425–2432, 2018.
- [44] S. Lin, R. Ji, C. Yan, B. Zhang, L. Cao, Q. Ye, F. Huang, and D. Doermann. Towards optimal structured cnn pruning via generative adversarial learning. In *Proceedings of the IEEE Conference on Computer Vision and Pattern Recognition*, pages 2790–2799, 2019.
- [45] J. Liu, J. Ye, and R. Fujimaki. Forward-backward greedy algorithms for general convex smooth functions over a cardinality constraint. In *International Conference on Machine Learning*, pages 503–511, 2014.
- [46] W. Liu, Y. Wen, Z. Yu, M. Li, B. Raj, and L. Song. Sphreface: Deep hypersphere embedding for face recognition. In *IEEE Conference on Computer Vision and Pattern Recognition*, pages 212–220, 2017.
- [47] Z. Liu, J. Li, Z. Shen, G. Huang, S. Yan, and C. Zhang. Learning efficient convolutional networks through network slimming. In *IEEE International Conference on Computer Vision*, pages 2736–2744, 2017.

- [48] Z. Liu, H. Mu, X. Zhang, Z. Guo, X. Yang, T. K.-T. Cheng, and J. Sun. Metapruning: Meta learning for automatic neural network channel pruning. In *IEEE International Conference on Computer Vision*, 2019.
- [49] Z. Liu, M. Sun, T. Zhou, G. Huang, and T. Darrell. Rethinking the value of network pruning. In *International Conference on Learning Representations*, 2019.
- [50] I. Loshchilov and F. Hutter. SGDR: stochastic gradient descent with warm restarts. In *International Conference on Learning Representations*, 2017.
- [51] J.-H. Luo, H. Zhang, H.-Y. Zhou, C.-W. Xie, J. Wu, and W. Lin. Thinet: pruning cnn filters for a thinner net. *IEEE Transactions on Pattern Analysis and Machine Intelligence*, 2018.
- [52] P. Molchanov, A. Mallya, S. Tyree, I. Frosio, and J. Kautz. Importance estimation for neural network pruning. In *IEEE Conference on Computer Vision and Pattern Recognition*, 2019.
- [53] P. Molchanov, S. Tyree, T. Karras, T. Aila, and J. Kautz. Pruning convolutional neural networks for resource efficient transfer learning. *arXiv preprint arXiv:1611.06440*, 3, 2016.
- [54] S. Moschoglou, A. Papaioannou, C. Sagonas, J. Deng, I. Kotsia, and S. Zafeiriou. Agedb: the first manually collected, in-the-wild age database. In *IEEE Conference on Computer Vision and Pattern Recognition Workshops*, pages 51–59, 2017.
- [55] V. Nair and G. E. Hinton. Rectified linear units improve restricted boltzmann machines. In *International Conference on Machine Learning*, pages 807–814, 2010.
- [56] Y. E. Nesterov. A method for solving the convex programming problem with convergence rate  $o(1/k^2)$ . In *Proceedings of the USSR Academy of Sciences*, volume 269, pages 543–547, 1983.
- [57] A. Paszke, S. Gross, F. Massa, A. Lerer, J. Bradbury, G. Chanan, T. Killeen, Z. Lin, N. Gimelshein, L. Antiga, et al. Pytorch: An imperative style, high-performance deep learning library. In *Advances in Neural Information Processing Systems*, pages 8024–8035, 2019.
- [58] Y. Rao, J. Lu, J. Lin, and J. Zhou. Runtime network routing for efficient image classification. *IEEE Transactions on Pattern Analysis and Machine Intelligence*, 2018.
- [59] M. Rastegari, V. Ordonez, J. Redmon, and A. Farhadi. Xnor-net: Imagenet classification using binary convolutional neural networks. In *European Conference on Computer Vision*, pages 525–542, 2016.
- [60] M. Sandler, A. Howard, M. Zhu, A. Zhmoginov, and L.-C. Chen. Mobilenetv2: Inverted residuals and linear bottlenecks. In *IEEE Conference on Computer Vision and Pattern Recognition*, pages 4510–4520, 2018.
- [61] F. Schroff, D. Kalenichenko, and J. Philbin. Facenet: A unified embedding for face recognition and clustering. In *IEEE Conference on Computer Vision and Pattern Recognition*, pages 815–823, 2015.
- [62] S. Sengupta, J.-C. Chen, C. Castillo, V. M. Patel, R. Chellappa, and D. W. Jacobs. Frontal to profile face verification in the wild. In *Winter Conference on Applications of Computer Vision*, pages 1–9, IEEE, 2016.
- [63] K. Simonyan and A. Zisserman. Two-stream convolutional networks for action recognition in videos. In *Advances in Neural Information Processing Systems*, pages 568–576, 2014.
- [64] K. Simonyan and A. Zisserman. Very deep convolutional networks for large-scale image recognition. In *International Conference on Learning Representations*, 2015.
- [65] V. Sindhwani, T. Sainath, and S. Kumar. Structured transforms for small-footprint deep learning. In *Advances in Neural Information Processing Systems*, pages 3088–3096, 2015.
- [66] S. Srinivas, A. Subramanya, and R. V. Babu. Training sparse neural networks. In *IEEE Conference on Computer Vision and Pattern Recognition Workshops*, pages 455–462, 2017.
- [67] R. K. Srivastava, K. Greff, and J. Schmidhuber. Training very deep networks. In *Advances in Neural Information Processing Systems*, pages 2377–2385, 2015.
- [68] Y. Sun, D. Liang, X. Wang, and X. Tang. Deepid3: Face recognition with very deep neural networks. *arXiv preprint arXiv:1502.00873*, 2015.
- [69] C. Szegedy, W. Liu, Y. Jia, P. Sermanet, S. Reed, D. Anguelov, D. Erhan, V. Vanhoucke, and A. Rabinovich. Going deeper with convolutions. In *IEEE Conference on Computer Vision and Pattern Recognition*, pages 1–9, 2015.
- [70] C. Tai, T. Xiao, X. Wang, and W. E. Convolutional neural networks with low-rank regularization. In *International Conference on Learning Representations*, 2016.
- [71] M. Tan and Q. Le. Efficientnet: Rethinking model scaling for convolutional neural networks. In *International Conference on Machine Learning*, pages 6105–6114, 2019.
- [72] M. Tan, I. W. Tsang, and L. Wang. Towards ultrahigh dimensional feature selection for big data. *Journal of Machine Learning Research*, 15(1):1371–1429, 2014.
- [73] M. Tan, I. W. Tsang, and L. Wang. Matching pursuit lasso part i: Sparse recovery over big dictionary. *IEEE Transactions on Signal Processing*, 63(3):727–741, 2015.
- [74] H. Wang, Y. Wang, Z. Zhou, X. Ji, D. Gong, J. Zhou, Z. Li, and W. Liu. Cosface: Large margin cosine loss for deep face recognition. In *IEEE Conference on Computer Vision and Pattern Recognition*, pages 5265–5274, 2018.
- [75] H. Wang, Q. Zhang, Y. Wang, and H. Hu. Structured probabilistic pruning for convolutional neural network acceleration. In *British Machine Vision Conference*, 2018.
- [76] L. Wang, Y. Xiong, Z. Wang, Y. Qiao, D. Lin, X. Tang, and L. Van Gool. Temporal segment networks: Towards good practices for deep action recognition. In *European Conference on Computer Vision*, pages 20–36, 2016.
- [77] W. Wen, C. Wu, Y. Wang, Y. Chen, and H. Li. Learning structured sparsity in deep neural networks. In *Advances in Neural Information Processing Systems*, pages 2074–2082, 2016.
- [78] T.-J. Yang, A. Howard, B. Chen, X. Zhang, A. Go, M. Sandler, V. Sze, and H. Adam. Netadapt: Platform-aware neural network adaptation for mobile applications. In *European Conference on Computer Vision*, pages 285–300, 2018.
- [79] J. Ye, X. Lu, Z. Lin, and J. Z. Wang. Rethinking the smaller-norm-less-informative assumption in channel pruning of convolution layers. In *International Conference on Learning Representations*, 2018.
- [80] Z. You, K. Yan, J. Ye, M. Ma, and P. Wang. Gate decorator: Global filter pruning method for accelerating deep convolutional neural networks. In *Advances in Neural Information Processing Systems*, 2019.
- [81] R. Yu, A. Li, C.-F. Chen, J.-H. Lai, V. I. Morariu, X. Han, M. Gao, C.-Y. Lin, and L. S. Davis. Nisp: Pruning networks using neuron importance score propagation. In *IEEE Conference on Computer Vision and Pattern Recognition*, pages 9194–9203, 2018.
- [82] X. Yuan, P. Li, and T. Zhang. Gradient hard thresholding pursuit for sparsity-constrained optimization. In *International Conference on Machine Learning*, pages 127–135, 2014.
- [83] R. Zeng, C. Gan, P. Chen, W. Huang, Q. Wu, and M. Tan. Breaking winner-takes-all: Iterative-winners-out networks for weakly supervised temporal action localization. *IEEE Transactions on Image Processing*, 28(12):5797–5808, 2019.
- [84] X. Zhang, J. Zou, K. He, and J. Sun. Accelerating very deep convolutional networks for classification and detection. *IEEE Transactions on Pattern Analysis and Machine Intelligence*, 38(10):1943–1955, 2016.
- [85] A. Zhou, A. Yao, Y. Guo, L. Xu, and Y. Chen. Incremental network quantization: Towards lossless cnns with low-precision weights. In *International Conference on Learning Representations*, 2017.
- [86] S. Zhou, Y. Wu, Z. Ni, X. Zhou, H. Wen, and Y. Zou. Dorefa-net: Training low bitwidth convolutional neural networks with low bitwidth gradients. *arXiv preprint arXiv:1606.06160*, 2016.
- [87] X. Zhu, W. Zhou, and H. Li. Improving deep neural network sparsity through decorrelation regularization. In *International Joint Conferences on Artificial Intelligence*, pages 3264–3270, 2018.
- [88] B. Zhuang, C. Shen, M. Tan, L. Liu, and I. Reid. Towards effective low-bitwidth convolutional neural networks. In *IEEE Conference on Computer Vision and Pattern Recognition*, pages 7920–7928, 2018.
- [89] B. Zhuang, C. Shen, M. Tan, L. Liu, and I. Reid. Structured binary neural networks for accurate image classification and semantic segmentation. In *IEEE Conference on Computer Vision and Pattern Recognition*, June 2019.
- [90] Z. Zhuang, M. Tan, B. Zhuang, J. Liu, Y. Guo, Q. Wu, J. Huang, and J. Zhu. Discrimination-aware channel pruning for deep neural networks. In *Advances in Neural Information Processing Systems*, pages 881–892, 2018.